

Decoding and Mitigating the Urban Heat Island Effect in Kolkata: A Two-Decade Geospatial and Remote Sensing Analysis

Advay Nathany

Abstract: The Urban Heat Island (UHI) effect, wherein urban areas exhibit significantly higher temperatures than their rural surroundings, has emerged as a critical environmental challenge in rapidly developing cities. In Kolkata, one of India's most densely populated and climatically vulnerable megacities, the intensification of UHI threatens thermal comfort, public health, and energy sustainability, particularly in dense informal settlements. This study provides a comprehensive two-decade (2005–2024) spatiotemporal assessment of UHI dynamics using multi-temporal Landsat datasets processed on the Google Earth Engine (GEE) platform. By integrating Land Surface Temperature (LST) and Normalised Difference Vegetation Index (NDVI) across seasonal snapshots (January, April, July and October), we identify and quantify thermal hotspots and vegetation loss at neighbourhood-level resolution. The analysis reveals a pronounced expansion of high-LST zones—most notably during the pre-monsoon season—concurrent with a progressive decline in NDVI values across the urban footprint. Seasonal patterns show April as the hottest period, January as the coolest, and October increasingly retaining elevated post-monsoon temperatures, indicating reduced thermal recovery. A correlation analysis between LST and NDVI confirms a strong inverse relationship, reinforcing the role of vegetation in mitigating surface heating. The findings highlight substantial SUHI (Surface Urban Heat Island) intensification over the past two decades, driven by rapid urbanisation, land cover transformation, and loss of green buffers. The study underscores the urgent need for integrated, climate-conscious urban planning strategies that prioritise vegetation restoration, green infrastructure expansion, and sustainable land use policies to mitigate UHI impacts and enhance urban resilience in Kolkata. The evidence generated from this two-decade geospatial analysis offers actionable intelligence for municipal authorities, urban planners, and environmental policymakers. Targeted interventions such as urban afforestation, riverfront greening, reflective surface mandates, and microclimate-sensitive zoning could substantially reduce heat exposure in vulnerable neighbourhoods. Incorporating these measures into Kolkata's climate adaptation framework will not only curb UHI intensity but also advance the city's alignment with the United Nations Sustainable Development Goals, particularly SDG 11 (Sustainable Cities and Communities) and SDG 13 (Climate Action).

Keywords: Urban Heat Island, Remote Sensing, Land Surface Temperature, Climate Resilience, Geospatial Analysis

1. Introduction

Urbanisation is among the most transformative anthropogenic processes of the modern era, exerting profound and often irreversible impacts on natural landscapes, surface energy balances, and atmospheric conditions across the globe (Shen et al., 2021; Shen et al., 2023). The spatial and material restructuring of cities, through the expansion of built-up areas, alteration of surface properties, and intensification of human activity, has fundamentally reshaped local climate systems. Among the various manifestations of this transformation, the Urban Heat Island (UHI) effect has emerged as one of the most studied yet persistently escalating environmental challenges (Joshi et al., 2024; Ren et al., 2023). The UHI phenomenon refers to the systematic elevation of temperatures in urban areas compared to their surrounding rural hinterlands, a result of complex interactions between urban morphology, material thermal properties, atmospheric processes, and anthropogenic heat emissions (Jayasinghe et al., 2024; Tabassum et al., 2025). Far from being a mere climatological anomaly, UHI represents a nexus issue with profound implications for public health, environmental sustainability, energy demand, and overall urban habitability, particularly in megacities of the Global South where rapid, unplanned growth converges with climatic vulnerability (Das et al., 2024; Joshi et al., 2024).

The physical mechanisms underlying the UHI effect are well-established in scientific literature. The progressive replacement of natural, permeable, and vegetated surfaces with impervious, heat-retaining materials such as asphalt,

concrete, and metal fundamentally alters the urban energy budget. These materials typically have higher heat capacities and lower albedo than natural surfaces, enabling them to absorb substantial solar radiation during the day and release it slowly during the night. The resulting diurnal thermal persistence leads to elevated nocturnal temperatures, exacerbating heat stress during critical rest periods. Vegetation loss further diminishes evapotranspiration, a natural cooling process that not only moderates air temperature but also enhances local humidity regulation. Additional anthropogenic heat sources, such as vehicular traffic, industrial activity, and residential energy consumption, directly contribute to thermal accumulation. Atmospheric pollutants and aerosols interact with incoming and outgoing radiation, modifying radiative balances and in some cases intensifying the UHI effect. These combined processes produce a thermal signature that is detectable both at the surface and in the lower atmosphere, with implications extending from local discomfort to broader climatic feedbacks (Aboulnaga et al., 2024; Islam et al., 2024).

Scholars have broadly distinguished between two primary forms of UHI: atmospheric UHIs, measured through air temperature differentials between urban and rural areas, and surface UHIs (SUHIs), which describe spatial variations in the radiometric temperature of the urban fabric as detected via thermal infrared (TIR) remote sensing (Jabbar et al., 2023; Shi et al., 2021). While atmospheric UHIs are typically quantified using ground-based weather stations or mobile transects, SUHIs offer the advantage of synoptic, spatially explicit measurement, enabling detailed mapping of intra-

urban thermal heterogeneity. For this reason, SUHI has become a focal point in remote sensing, based urban climate studies, particularly in contexts where in-situ temperature networks are sparse or absent (Almeida et al., 2021).

Remote sensing has emerged as a powerful and versatile tool for monitoring environmental parameters across land, air, and water systems, enabling consistent, large-scale, and multi-temporal assessments of ecological and climatic processes (Agarwal et al., 2021; Panday et al., 2024; Agarwal et al., 2024; Singh et al., 2025). Its capacity to integrate spectral, thermal, and radar observations makes it indispensable for detecting changes in vegetation, surface temperature, hydrology, and atmospheric conditions (Panday et al., 2025; Das et al., 2024; Vishvendra et al., 2024).

Land Surface Temperature (LST) is a cornerstone parameter in SUHI research. Defined as the radiometric “skin” temperature of the land surface, LST can be derived from satellite-borne TIR sensors and has been widely employed to quantify thermal patterns in urban environments (Li et al., 2023; Anand et al., 2025; Kumar et al., 2021). The LST metric captures the aggregate thermal response of different land cover types, from high-reflectance rooftops to dense tree canopies, enabling both spatial pattern recognition and temporal trend analysis. LST studies frequently incorporate vegetation metrics to contextualise observed temperature variations. Among these, the Normalised Difference Vegetation Index (NDVI) remains the most widely used. NDVI, calculated from the contrast between red and near-infrared reflectance, is a robust indicator of vegetation presence and condition. Numerous studies have documented the inverse correlation between NDVI and LST, wherein higher vegetation density and health correspond to lower surface temperatures, largely due to shading and evapotranspiration effects (Raufu., 2024; Mohanasundaram et al., 2023). Conversely, indices such as the Normalised Difference Built-up Index (NDBI) have proven useful in isolating impervious surface areas, which tend to exhibit elevated LST values. The integration of these indices with LST offers a multi-dimensional analytical framework capable of diagnosing the relative influence of vegetative cover loss and built-up expansion on urban thermal patterns.

The UHI effect has been the subject of extensive research globally, with foundational works by Oke (1995), and Voogt and Oke (2003) elucidating the physical basis and measurement methodologies. More recent studies have leveraged medium- to high-resolution satellite platforms, such as the Landsat series and MODIS, to capture decadal trends in SUHI intensity and spatial extent. In India, notable work has been conducted in cities such as Delhi, Mumbai, and Ahmedabad, revealing strong links between SUHI intensification, rapid urban sprawl, and declining green cover (Taloor et al., 2024; Shahfahad et al., 2022; Ahmad et al., 2024)). However, the bulk of these studies are either temporally restricted, often covering less than a decade, or spatially coarse, relying on moderate-resolution sensors that cannot resolve neighbourhood-scale variability. Moreover, while Kolkata is one of India’s most densely populated and climatically exposed metropolitan regions, the number of longitudinal, high-resolution

SUHI studies in this urban context remain surprisingly limited. This scarcity is particularly striking given Kolkata’s unique combination of high population density, extensive informal settlements, monsoon-dominated climate, and ongoing land use transformations.

Kolkata’s urban expansion over the past two decades has been characterised by both horizontal sprawl into peri-urban areas and vertical densification within its historic core (Mondal & Banerjee., 2021; Chakraborty et al., 2021). This growth has coincided with measurable reductions in vegetated open spaces and an intensification of built-up impervious surfaces. The city’s humid subtropical climate, with its pronounced pre-monsoon heat periods and high post-monsoon humidity, amplifies heat stress risks, particularly for vulnerable populations lacking access to cooling infrastructure. The interaction between SUHI patterns and socio-economic vulnerability remains underexplored in the Kolkata context, representing a critical knowledge gap with direct policy implications.

The present study addresses these gaps through a comprehensive, two-decade analysis (2005–2025) of SUHI dynamics in Kolkata, using multi-source Landsat thermal datasets processed within the cloud-computing environment of Google Earth Engine (GEE). The methodological novelty lies in the integration of temporally consistent LST retrievals with NDVI derived land cover indicators, enabling a seasonally stratified, neighbourhood-scale diagnosis of SUHI patterns. GEE’s capacity for large-scale data processing allows the application of robust temporal compositing, statistical trend detection, and spatial autocorrelation analyses across a 20-year timespan.

From a sustainability perspective, the relevance of this work is manifold. The UHI effect is not merely a thermal anomaly; it is a critical factor in urban energy demand, greenhouse gas emissions, air quality deterioration, and public health outcomes. In hot and humid climates such as Kolkata’s, elevated nighttime temperatures associated with UHI can significantly increase cooling energy consumption, contributing to peak electricity loads and, in turn, higher emissions from thermal power plants. Vulnerable communities, particularly those in informal housing with poor thermal insulation, face heightened risks of heat-related morbidity and mortality. By providing high-resolution, temporally robust maps of SUHI hotspots, this research supports the strategic deployment of nature-based solutions such as rooftop greening, urban forestry, and water-sensitive landscaping. It also informs the application of reflective and biomimetic surface materials in priority zones, contributing to broader climate resilience strategies.

This study is also aligned with the United Nations’ Sustainable Development Goals (SDGs), particularly SDG 11 (Sustainable Cities and Communities) and SDG 13 (Climate Action). The methodological framework, grounded in open-source tools and datasets, offers scalability and replicability for other climate-stressed cities in the Global South, fostering knowledge transfer and collaborative urban resilience planning. Furthermore, by explicitly linking geospatial analysis with environmental justice considerations—identifying areas where high SUHI intensity intersects with

socio-economic vulnerability- the research contributes to a more equitable distribution of climate adaptation resources.

While the UHI effect has been extensively documented in the literature, its long-term, fine-scale evolution in Kolkata remains insufficiently understood, particularly in relation to vegetation dynamics, built-up expansion, and vulnerable population exposure. This study advances the field by combining two decades of high-resolution Landsat-derived LST, NDVI, and NDBI metrics with in-situ validation, processed via GEE's scalable infrastructure. The resulting insights are intended not only to deepen the scientific understanding of SUHI processes in a major South Asian metropolis but also to inform actionable, spatially targeted interventions for thermal equity and sustainability. Through its integration of advanced remote sensing analytics, field validation, and climate resilience framing, the research offers a novel contribution to both the academic literature and the policy discourse on sustainable urban futures in the face of accelerating global change.

2. Study Area

Kolkata, the capital city of the Indian state of West Bengal, is one of the largest and most densely populated metropolitan regions in India, with an estimated population exceeding 14 million in its urban agglomeration (Basu et al., 2025; Chakraborty et al., 2021). Located in the eastern part of India, Kolkata lies between 22°28' N to 22°38' N latitude and 88°17' E to 88°23' E longitude, covering an area of approximately 185 km² within the municipal limits and over 1,800 km² in the metropolitan region.

Kolkata is situated in the Ganges-Brahmaputra delta, on the eastern bank of the Hooghly River, a distributary of the Ganges. Its elevation is low, averaging only 9 meters above sea level, which makes the city highly susceptible to flooding during extreme rainfall events and cyclonic storms. The city's proximity to the Bay of Bengal influences its climate, which is classified as tropical wet-and-dry (Chatterjee et al., 2022; Maity et al., 2022).

The climate is characterized by four distinct seasons. The winter (December–February), is characterised by mild temperatures, low humidity, and the lowest average LST values. The Pre-Monsoon or Summer (March–May) observes high temperatures, peak LST values, and frequent heatwaves. This is then followed by the Monsoon (June–September), with heavy rainfall, high humidity, and moderated LST due to cloud cover. Finally, the Post- Monsoon period (October–November) witnesses gradual temperature decline, and relatively high residual soil moisture. Average annual rainfall exceeds 1,600 mm, with over 75% occurring during the monsoon. Average monthly maximum temperatures range from 26°C in January to over 38°C in May, though LST values during peak summer can exceed 45°C in built-up areas. Kolkata's urban form reflects a dense core of historical development surrounded by rapidly expanding suburban zones. The central business district and older residential areas exhibit narrow streets, limited vegetation, and high-rise concrete structures create an environment conducive to UHI formation. Peripheral regions are undergoing rapid transformation from agricultural and open land to built-up

areas, often without adequate green space planning (Halder et al., 2021; Maltare et al., 2024).

The major land cover categories in Kolkata comprise built-up areas, including high-density residential neighbourhoods, commercial hubs, and industrial zones; vegetated areas, such as parks, roadside plantations, and remnant agricultural plots that contribute to urban cooling; water bodies, notably the Hooghly/Ganges River along with lakes, ponds, and canal networks that offer localized thermal regulation; and bare soil or open land, encompassing construction sites and undeveloped parcels that often act as heat-retaining surfaces due to their low albedo and lack of vegetative cover. Over the past two decades, Kolkata has witnessed significant conversion of vegetated and open areas into impervious surfaces, driven by population growth, economic activity, and infrastructural expansion.

Rationale for Selecting Kolkata for UHI Analysis: Kolkata presents a unique and urgent case for UHI research for several reasons. Its climate vulnerability (due to its low lying location), dense population, and exposure to both heatwaves and extreme rainfall events make it highly sensitive to climate change impacts. Additionally, Rapid Land Cover Change caused by accelerated urban expansion has markedly reduced vegetative cover, exacerbating thermal stress. As stated earlier, this has led to major public health concerns, especially given the Increasing frequency of heatwaves which poses severe health risks, particularly to vulnerable populations living in informal settlements with limited access to cooling infrastructure. being a megacity, there is a lack of long-term, high-resolution studies on UHI patterns in Kolkata, limiting the evidence base for urban heat mitigation policies. By selecting Kolkata as the study area, this research will not only address a critical literature gap but also provide decision-support tools to urban planners, enabling the design of climate-resilient infrastructure and nature-based solutions tailored to the city's unique environmental and socio-economic context.

3. Data and Methodology

The analysis utilised multi-temporal satellite datasets from the Landsat series, including Landsat 5 TM, Landsat 7 ETM+, Landsat 8 OLI/TIRS, and Landsat 9 OLI/TIRS, covering the years 2005, 2010, 2015, 2020, and 2024 (Hemati et al., 2021; Wulder et al., 2022). Images were accessed via the Google Earth Engine (GEE) platform, which enabled streamlined data retrieval, cloud masking, and reproducible geospatial processing. To represent seasonal variation, four months–January (winter), April (pre-monsoon), July (monsoon), and October (post-monsoon)– were selected for each study year. Administrative boundary shapefiles for Kolkata Municipal Corporation were sourced from the Survey of India and OpenStreetMap, ensuring accurate georeferencing and spatial clipping of imagery to the study area.

Radiometric and atmospheric corrections were applied to all imagery using the LEDAPS algorithm for Landsat 5/7 and the LaSRC algorithm for Landsat 8/9. Cloud and cloud-shadow pixels were removed using the CFMask algorithm, and images were subset to the municipal boundary to exclude peri-urban and rural regions. Land Surface Temperature

(LST) was retrieved from thermal infrared bands using the radiative transfer equation (RTE) method, involving conversion of digital numbers to spectral radiance, transformation to at-sensor brightness temperature, and surface emissivity correction derived from NDVI-based emissivity estimation. Seasonal LST maps were generated for all years to enable both spatial and temporal comparisons of surface thermal patterns.

Vegetation cover was quantified using the Normalized Difference Vegetation Index (NDVI), calculated from the red and near-infrared bands. NDVI values were classified into dense vegetation (>0.5), moderate vegetation (0.25–0.5), sparse vegetation (0–0.25), degraded or barren land (<0), and water bodies (distinct negative values). These vegetation maps were examined in conjunction with LST maps to explore vegetation–temperature interactions across seasons and years.

Pearson's correlation coefficients were computed between NDVI and LST for each month and year to assess the statistical strength and direction of relationships, while scatter plots and pairwise correlation matrices were used for visualisation. Temporal analysis was carried out to identify persistent high-temperature zones and assess their linkages to specific land cover transitions. Spatial hotspot detection was implemented to map statistically significant thermal anomalies, thereby enabling a clear understanding of how urban growth and vegetation loss have shaped the UHI patterns in Kolkata over the past two decades.

4. Results and Discussions

a) Spatiotemporal Patterns of LST and NDVI (2005–2024)

The twenty-year geospatial analysis of Land Surface Temperature (LST) and Normalised Difference Vegetation Index (NDVI) in Kolkata reveals a pronounced and sustained intensification of the Surface Urban Heat Island (SUHI) effect, coupled with a significant decline in vegetative cover. This progression has not been linear but exhibits identifiable accelerations in certain periods, reflecting both macro-scale urbanisation trends and localised land-use transitions. In 2005, spatially, the city's thermal landscape displayed clear differentiation between cooler, vegetation-rich zones and high-temperature clusters (Figure 1). Elevated LST zones ($\geq 40^{\circ}\text{C}$) were largely confined to industrial clusters in the eastern and northern parts of the city, major transport corridors such as the Eastern Metropolitan Bypass, and the dense commercial core around B.B.D. Bagh and Esplanade. Pre-monsoon April consistently emerged as the hottest period, with large parts of the urban fabric exceeding 40°C , whereas January remained the coolest month, with most wards registering below 26°C . These findings align with earlier urban thermal studies in South Asian megacities, where peak pre-monsoon months intensify surface heat stress due to low atmospheric humidity, clear skies, and intense solar radiation (Kotharkar et al., 2018; Sarif et al., 2022; Hossain et al., 2015).

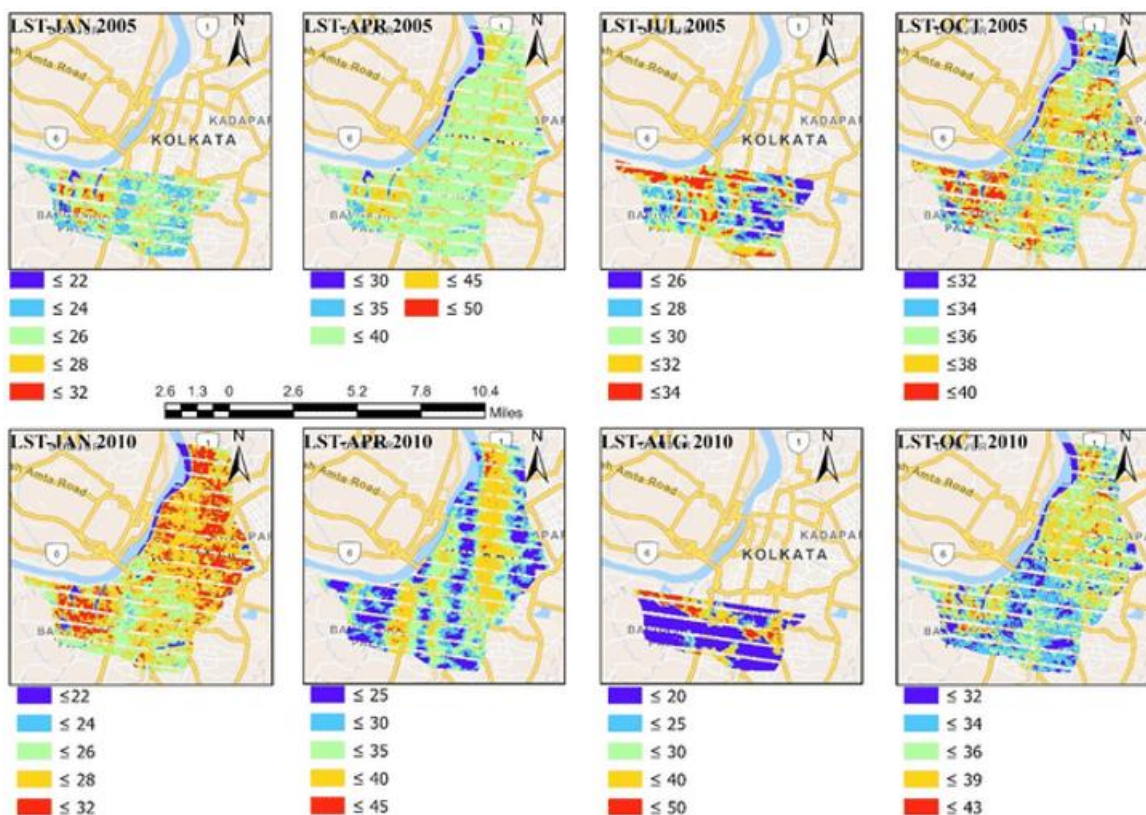


Figure 1: Seasonal distribution of Land Surface Temperature (LST) in Kolkata for the years 2005 and 2010, derived from multi-temporal Landsat imagery. The maps depict January (winter), April (pre-monsoon), July/August (monsoon peak), and October (post-monsoon) conditions. Colour gradients represent temperature classes in $^{\circ}\text{C}$, illustrating the expansion of high-temperature zones—particularly during the pre-monsoon season—and the spatial persistence of thermal hotspots over time.

NDVI patterns from 2005 (Figure 2) showed a still-resilient green infrastructure, with moderate to high vegetation cover (≥ 0.25) along the Hooghly River, peri-urban agricultural fields, institutional campuses, and scattered parks such as the Maidan. These areas acted as thermal sinks, suppressing local

LST by several degrees. However, the early signs of vegetation stress and conversion to impervious surfaces were evident in eastern reclaimed wetland areas and fringe settlements, where NDVI values had already dropped to ≤ 0.0 .

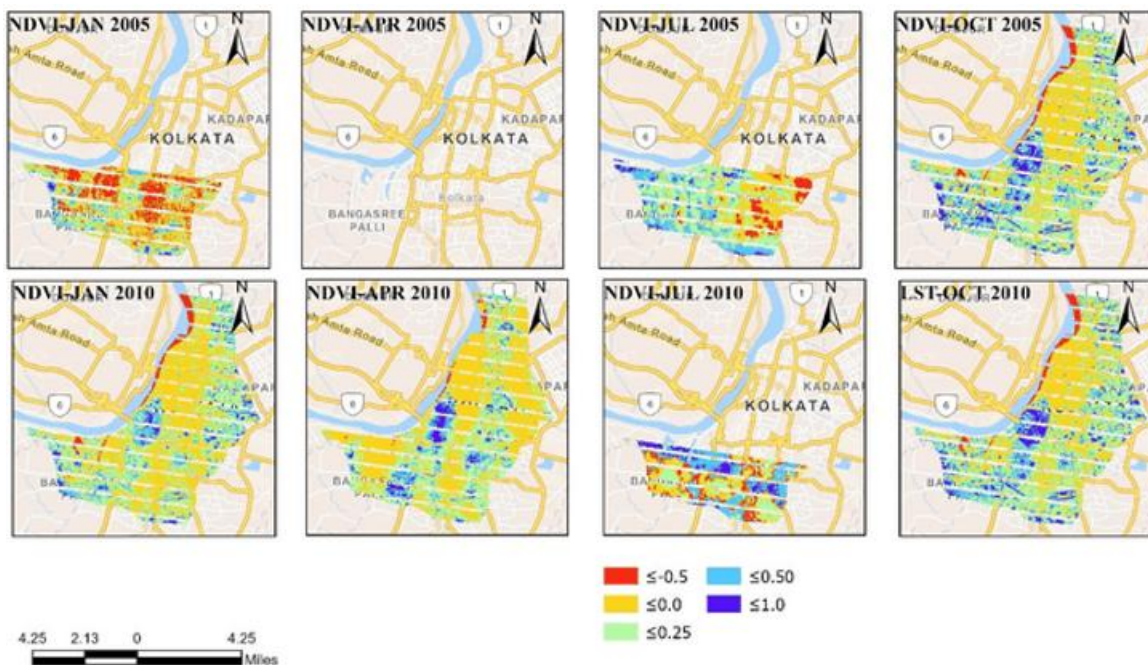


Figure 2: Seasonal distribution of the Normalised Difference Vegetation Index (NDVI) in Kolkata for the years 2005 and 2010, derived from multi-temporal Landsat imagery. The maps represent January (winter), April (pre-monsoon), July (monsoon peak), and October (post-monsoon) vegetation conditions. Colour gradients indicate NDVI ranges, highlighting the spatial variation in vegetative cover, with notable declines in dense vegetation zones and increasing areas of low or negative NDVI, particularly in the central and industrial urban core between 2005 and 2010.

By 2010, the spatial expansion of high-LST zones was unmistakable (Figure 1). April maxima surpassed 45°C in several wards, particularly in the eastern industrial corridor and peripheral neighbourhoods undergoing land conversion from agriculture to built-up land. This intensification coincided with Kolkata's rapid peri-urban growth phase, driven by both formal real estate development and unplanned settlement expansion. The NDVI data for 2010 reflected an accelerating loss of vegetation, particularly in central and eastern sectors (Figure 2). Large swathes of NDVI ≤ 0.0 emerged where impervious materials had replaced vegetated plots. The decline was especially stark in reclaimed wetland areas, confirming ecological warnings about the environmental costs of encroaching on these natural buffers.

The 2015 datasets mark a critical inflection point (Figure 3 and Figure 4). April LST values reached $\geq 45^{\circ}\text{C}$ across extensive areas, while October, which traditionally allowed for post-monsoon thermal recovery, began showing persistent heat pockets. This persistence was particularly visible in high-density informal settlements and industrial belts, suggesting a shift from seasonal heat extremes to prolonged thermal stress.

NDVI trends during this period underscored a substantial depletion of vegetative buffers in newly urbanised peripheries. Many of these areas had transitioned within a decade from semi-rural landscapes to dense, unshaded built environments. The loss of green cover was not merely quantitative but also qualitative: older, mature tree canopies were replaced by sparse or ornamental greenery incapable of delivering equivalent cooling benefits.

By 2020, the intensification of SUHI was extreme (Figure 3 and Figure 4). April LST exceeded 50°C in several peri-urban fringes, a temperature range associated with severe heat stress and potential public health emergencies. October retained heat levels similar to pre-2010 April averages, underscoring the diminishing amplitude of seasonal temperature recovery. NDVI ≤ 0.0 now dominated much of the urban footprint, especially in eastern, northern, and southern industrial belts and low-income housing clusters. The remaining vegetated patches were highly fragmented, reducing their cooling influence through loss of connectivity and scale.

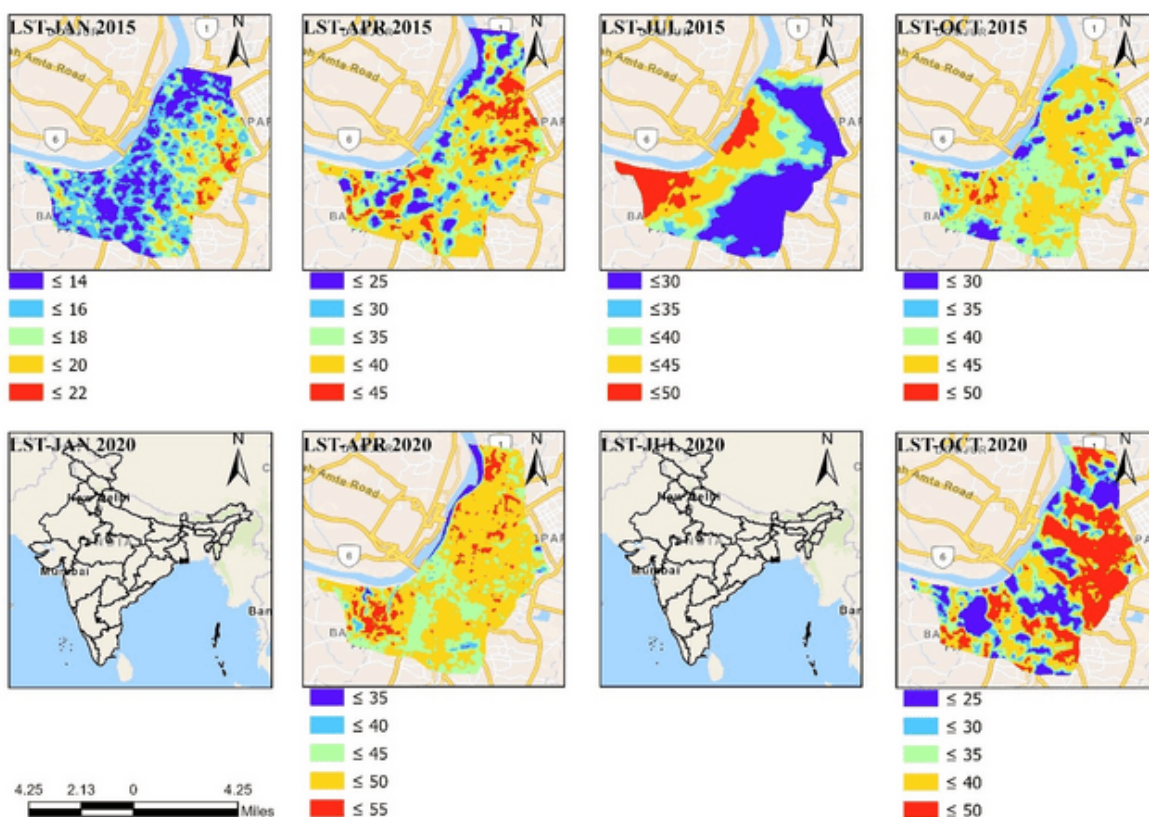


Figure 3: Seasonal variation in Land Surface Temperature (LST) across Kolkata for the years 2015 and 2020, derived from multi-temporal Landsat imagery. The maps depict January (winter), April (pre-monsoon), July (monsoon peak), and October (post-monsoon) thermal profiles. Colour gradients represent LST ranges, illustrating spatial heterogeneity in surface heating.

Notable patterns include intense pre-monsoon thermal hotspots in central and peri-urban areas, as well as seasonal cooling effects during the monsoon. A clear intensification of high-LST zones is visible from 2015 to 2020, indicating the progression of the Surface Urban Heat Island (SUHI) effect.

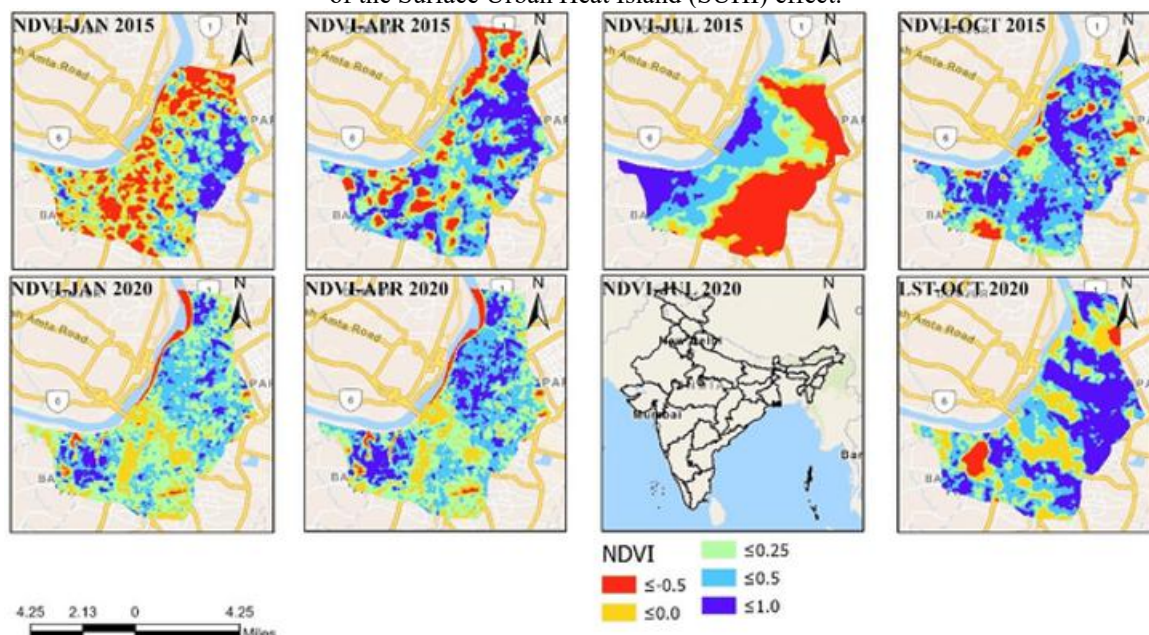


Figure 4: Seasonal distribution of the Normalised Difference Vegetation Index (NDVI) for Kolkata during 2015 and 2020, derived from Landsat datasets. The maps depict January (winter), April (pre-monsoon), July (monsoon peak), and October (post-monsoon) vegetation conditions. Colour gradients represent NDVI values, with higher values (blue–purple) indicating dense vegetation and lower values (red–orange) indicating sparse or degraded vegetation. The comparison reveals a marked decline in vegetation health and density in several urban cores between 2015 and 2020, especially in pre-monsoon and post-monsoon periods, contributing to intensified SUHI patterns.

The 2024 maps represent the culmination of this two-decade trajectory (Figure 5). April LST peaks approached $\sim 51^{\circ}\text{C}$ in the city's densest cores, including Burrabazar, Tangra, and large swathes of Salt Lake's commercial sectors. NDVI >0.25 survived only along limited riverbank stretches, institutional campuses, and elite residential enclaves. October temperatures frequently reached $\geq 44^{\circ}\text{C}$ in inner-city wards, indicating a systemic thermal inertia wherein heat retention through the monsoon season neutralises the historical cooling effect of rainfall and increased humidity.

Seasonal patterns across the entire period show three consistent observations. First, January remains the coolest month, though the gap between January minima and April maxima has widened, indicating stronger seasonal contrasts. Second, April's pre-monsoon heat has not only intensified but expanded spatially to encompass larger urban and peri-urban areas. Third, October increasingly reflects a delayed cooling pattern, with residual heat persisting well into the post-monsoon period. These seasonal changes underscore the compounded role of land cover change and urban morphology in altering the city's thermal regime.

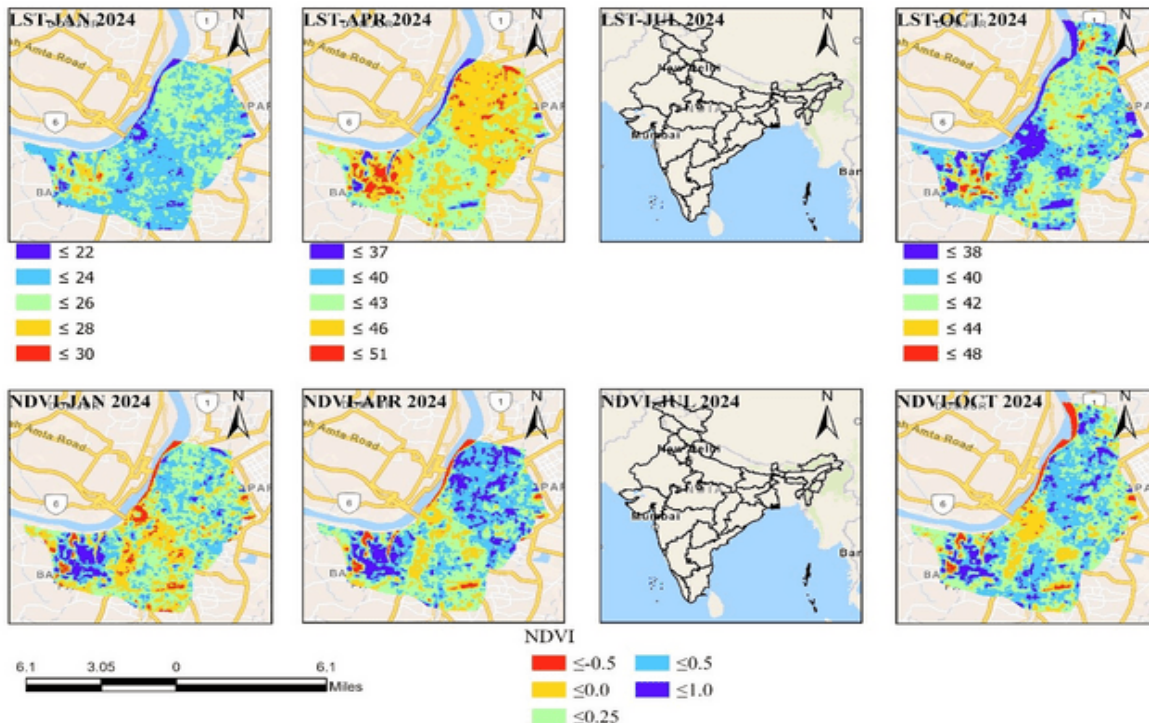


Figure 5: Seasonal distribution of Land Surface Temperature (LST) and Normalised Difference Vegetation Index (NDVI) for Kolkata in 2024, derived from Landsat datasets. The maps illustrate January (winter), April (pre-monsoon), July (monsoon peak), and October (post-monsoon) conditions. LST maps (top row) indicate significant seasonal temperature variability, with the highest surface heating during the pre-monsoon period and moderate cooling during the monsoon. NDVI maps (bottom row) depict vegetation health, with higher values (blue–purple) corresponding to dense vegetation and lower values (red–orange) indicating sparse or stressed vegetation. The spatial relationship between elevated LST and reduced NDVI highlights areas of intensified Surface Urban Heat Island (SUHI) effects in 2024.

b) Interpretation and Implications for SUHI Dynamics and Sustainability

The longitudinal results offer compelling evidence that Kolkata's SUHI effect is both intensifying and structurally embedded within the city's evolving urban fabric. The observed trends can be interpreted through three interlinked drivers: (a) land cover transformation, (b) thermal storage and retention capacity of built surfaces, and (c) disruption of urban ecological buffers.

Land cover change has been the most visible driver. The replacement of agricultural fields, wetlands, and tree-lined avenues with impervious surfaces: concrete, asphalt, and metal roofing, has altered the surface energy balance, reducing albedo and increasing heat storage capacity. In Kolkata's case, the reclamation of wetlands, documented extensively since the 1990s, has had a dual impact: removing high-cooling-capacity ecological zones and replacing them

with industrial or residential structures that actively store and radiate heat.

Thermal storage properties have also shifted with the densification of the built environment. High-rise, closely spaced buildings create urban canyons that trap heat and reduce wind ventilation, amplifying nocturnal temperature retention. The persistence of elevated October temperatures post-2015 reflects this structural change. Where previously monsoonal rains would flush heat from urban surfaces, the current morphology retains absorbed radiation, creating a year-round baseline of elevated surface temperatures.

Ecological disruption has compounded these effects. The loss of large, contiguous vegetated areas reduces evapotranspiration, the primary natural cooling mechanism in humid tropical climates. NDVI declines in peri-urban zones are particularly concerning because these transitional areas historically acted as buffers that moderated heat inflow into

the urban core. Their disappearance means that heat generated in the periphery now flows unimpeded into the city centre, contributing to the spatial expansion of SUHI.

From a sustainability standpoint, the implications are severe. Rising pre-monsoon LST extremes directly increase public health risks, particularly for the urban poor, who often live in poorly ventilated dwellings without access to mechanical cooling. The correlation between low NDVI and high LST zones indicates that these vulnerable populations are also those most deprived of natural cooling infrastructure, raising pressing environmental justice concerns.

Mitigation strategies must therefore go beyond traditional green cover restoration. While urban afforestation, rooftop gardens, and vertical greening are essential, they must be implemented alongside high-albedo building materials, permeable pavements, and urban ventilation corridor design. Furthermore, land-use zoning policies need to integrate SUHI risk mapping into their regulatory framework, prioritising the preservation of remaining wetlands and peri-urban green spaces.

The findings also have regional and global resonance. Kolkata's SUHI trajectory reflects the experience of many rapidly urbanising tropical megacities, where population growth, economic development, and land scarcity create powerful incentives for ecological conversion. The hybrid methodology employed here, combining multi-temporal LST and NDVI mapping with seasonal correlation analysis, provides a replicable framework for cities in the global South seeking to align heat mitigation with Sustainable Development Goals (SDGs), particularly SDG 11 (Sustainable Cities and Communities) and SDG 13 (Climate Action).

c) Seasonal NDVI–LST Correlation Analysis

The seasonal correlation matrix between NDVI and LST provides robust statistical validation of the inverse vegetation–temperature relationship observed in the spatial maps (Figure 6). In most seasons, NDVI is negatively correlated with LST, affirming vegetation's role in reducing surface heat through shading and evapotranspiration.

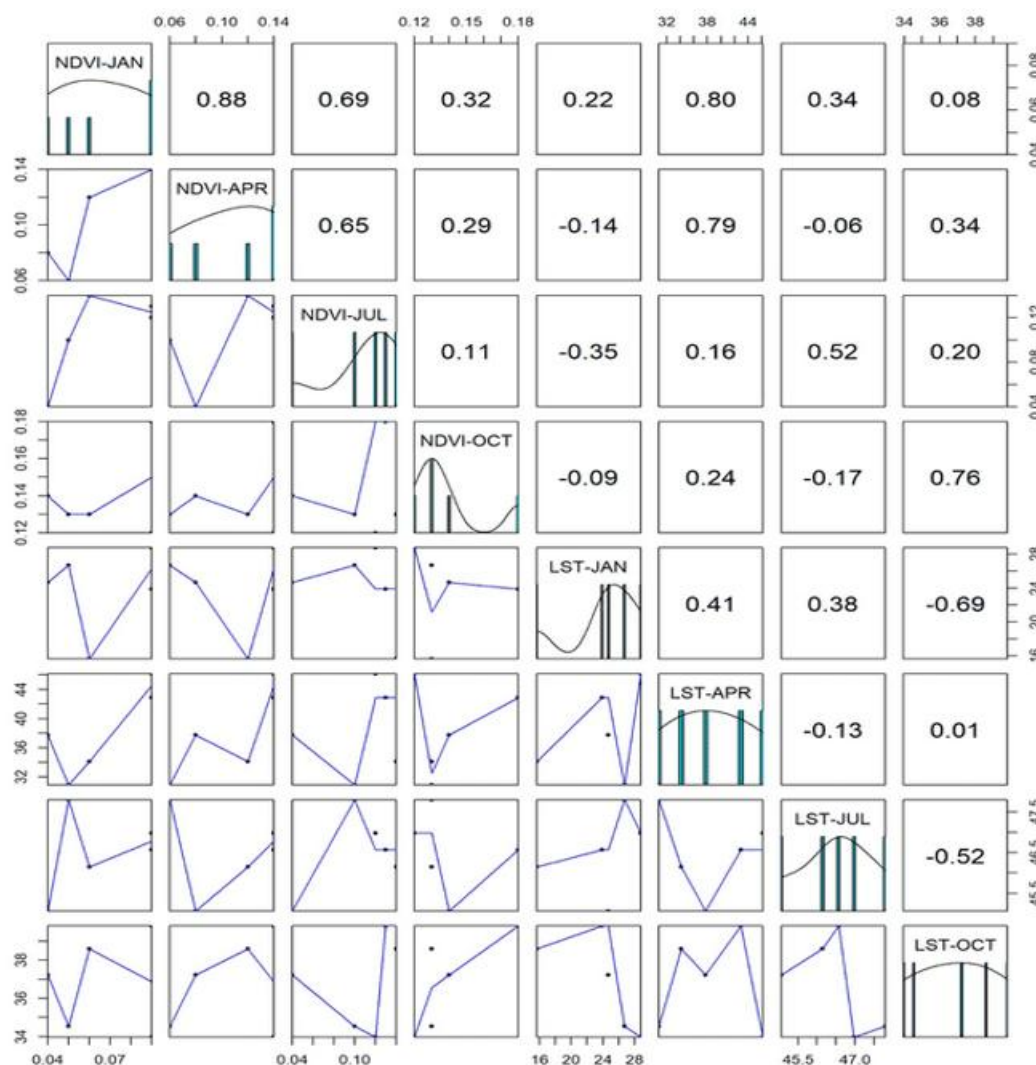


Figure 6: Pairwise correlation matrix between seasonal Normalised Difference Vegetation Index (NDVI) and Land Surface Temperature (LST) for Kolkata in 2024. The diagonal panels display the distribution (histograms and density plots) of each variable. The upper triangular panels present Pearson's correlation coefficients, indicating the strength and direction of linear relationships between NDVI and LST for January, April, July, and October. The lower triangular panels depict scatterplots with trend lines, showing the seasonal variability and inverse NDVI–LST relationship, particularly evident during the monsoon (July) and post-monsoon (October) periods.

In January, the correlation between NDVI and LST is moderately strong ($r = -0.69$), despite it being the coolest month of the year. This reflects the fact that even in winter, vegetated areas are systematically cooler than non-vegetated surfaces. April, however, exhibits a weaker NDVI–LST correlation ($r = -0.13$). This suggests that during peak pre-monsoon heat, vegetation's cooling effect is attenuated by environmental stress factors such as high vapor pressure deficit, soil dryness, and intense solar radiation, alongside the overwhelming radiative load absorbed by impervious surfaces.

July, representing the monsoon peak, shows a stronger negative correlation ($r = -0.52$). With ample moisture availability, vegetation in July actively contributes to lowering LST, especially in peri-urban zones where agricultural fields and wetlands persist. Nonetheless, the correlation remains moderate rather than strong, indicating that urban morphology and built-up density still exert a dominant influence on LST, even in periods of maximal greenness. October presents an even weaker negative correlation ($r = -0.17$), reflecting persistent heat storage in built-up zones despite partial vegetation recovery post-monsoon. This underscores the “thermal memory” effect of urban materials, where the residual heat from the pre-monsoon and monsoon seasons is retained and slowly released over weeks.

Autocorrelation values also yield valuable insights. NDVI autocorrelations are high between January and April ($r = 0.88$) and between January and October ($r = 0.80$), indicating stable spatial patterns in vegetation cover. Areas with low NDVI in one season tend to remain vegetation-poor throughout the year. LST autocorrelations between January and April ($r = 0.41$) and January and October ($r = 0.38$) confirm the persistence of thermal hotspots across seasons, while the negative correlations between LST in July and other months reflect the transient cooling effect of monsoonal conditions. Together, these statistical patterns reinforce the conclusion that vegetation, while an important cooling factor, cannot singlehandedly counteract the structural and material drivers of SUHI in a city like Kolkata. The results point toward an

integrated mitigation strategy that combines ecological restoration with urban design interventions and targeted policy action.

The integrated spatiotemporal mapping, statistical correlation analysis, and interpretive synthesis collectively underscore the structural permanence and seasonal variability of Kolkata's SUHI phenomenon. Over two decades, the expansion of impervious surfaces, disruption of peri-urban ecological buffers, and densification of built-up zones have shifted the city's thermal regime from a seasonally moderated pattern to one marked by persistent, year-round heat stress. While NDVI trends confirm the progressive erosion of vegetation's cooling potential, the seasonal correlation dynamics reveal that even in high-greenness months, urban form and material composition continue to dictate thermal outcomes. This evidence positions the SUHI challenge not merely as an environmental issue, but as a governance and urban planning imperative, requiring integration of climate-responsive zoning, ecological preservation, and heat-resilient design principles. In doing so, the findings provide both a granular empirical record and a replicable methodological framework for tropical megacities confronting parallel climate urbanisation feedback loops.

d) Evidence-Based Mitigation Strategies and Implementation Roadmap

Ranking Mitigation Interventions

Based on the spatial and temporal patterns revealed by this study, particularly the seasonal intensification of LST and the weakening NDVI–LST relationship during pre-monsoon extremes, an evidence-based mitigation framework was developed for Kolkata. Each strategy below is informed by empirical studies from comparable tropical and subtropical Asian cities and ranked according to (A) expected surface cooling potential, (B) feasibility in Kolkata's socio-economic context, and (C) co-benefits for health, biodiversity, and energy systems. The quantitative effect ranges represent conservative, literature-consistent averages for surface or near-surface air-temperature reductions observed in field and remote-sensing studies.

Table 4.1: Ranked Mitigation Interventions for Kolkata

Rank	Intervention	Expected Local Surface LST Reduction (approx.)	Spatial Target	Feasibility	Key Co-Benefits
1	Wetland / Hooghly Riverbank Restoration & Peri-Urban Greening	0.8-3.0°C near wetlands and riparian zones	Reclaimed eastern wetlands, Hooghly riverbanks, peri-urban agricultural fringe	Medium (requires land-use reform and compensation)	Flood buffering, biodiversity corridors, carbon sequestration, urban cooling
2	Urban Canopy & Street-Tree Corridors	0.5-2.5°C under canopy; up to 1 °C at neighborhood scale	Burrabazar, Tangra, Eastern Bypass, industrial corridors	High (feasible via civic and NGO programs)	Shading, air-quality improvement, pedestrian comfort, heat-stress reduction
3	Cool Roofs + Rooftop Greening	Roof-surface $\Delta T = 9-13 °C$; indoor $\Delta T = 0.5-2.5 °C$	Salt Lake commercial core, markets, informal settlements	High (supported by subsidies and community labor)	Energy savings, reduced cooling demand, green-jobs potential
4	High-Albedo Pavements / Reflective Coatings	Surface $\Delta T = 1-5 °C$; local air $\Delta T \leq 1 °C$	Market plazas, transit hubs, pedestrian corridors	Medium (maintenance required)	Pedestrian thermal comfort, reduced material fatigue
5	Urban Ventilation Corridors & Zoning Reform	Air-temperature $\Delta T = 0.5-1.5 °C$	Dense historic cores with narrow street canyons	Low-Medium (planning-intensive)	Air-flow enhancement, pollutant dispersion, improved humidity control
6	Water-Sensitive Landscaping (Ponds,...	0.5-2.0°C within 50-150 m of features	Parks, campuses, peri-urban open spaces	Medium (requires water-quality management)	Flood mitigation, groundwater recharge, biodiversity

	Bioswales, Green Infrastructure)				
7	Industrial Energy Efficiency & Anthropogenic-Heat Reduction	Ambient $\Delta T \leq 0.5$ °C (city-scale)	Industrial and transport corridors	Medium (regulatory incentives required)	Reduced GHGs, lower peak loads, improved local air quality
8	Passive Building Design & Envelope Upgrades	Indoor $\Delta T = 1-3$ °C	Dense residential wards and school	Medium (retrofit cost, design awareness)	Thermal comfort, health benefits, energy resilience

All temperature ranges derive from empirical studies in tropical or subtropical urban environments (Athukorala et al., 2025; Li et al., 2024; Budhiyanto et al., 2024; Cheela et al., 2021; Luo et al., 2024; Wang et al., 2022; Xie et al., 2016; Priya et al., 2024).

Priority Phasing and Spatial Targeting Plan

To translate the ranked mitigation strategies into measurable climate action, a phased implementation roadmap is proposed for Kolkata, structured around short-, medium-, and long-term horizons. The framework aims to balance ecological restoration with engineered cooling, ensuring that interventions are both scientifically verifiable and socio-economically feasible. Each phase is designed to progressively expand spatial coverage and institutional depth—beginning with demonstration pilots, advancing through city-scale ecological programs, and culminating in structural urban planning reform.

Phase 0: Immediate (0-2 years) - Pilot Hotspot Rollout and Validation.

The first phase focuses on establishing demonstrable, data-backed results in high-priority thermal zones identified through the Landsat analysis. Three wards—Burrabazar, Tangra, and Salt Lake—are selected as representative pilot areas due to their consistently elevated pre-monsoon surface temperatures (often exceeding 50 °C) and contrasting land-use characteristics. In these zones, a coordinated program combining cool-roof coatings, reflective pavement materials, and continuous street-tree corridors will be implemented under municipal supervision. The Kolkata Municipal Corporation (KMC), in collaboration with the West Bengal Pollution Control Board and community partners, will oversee these interventions. Each pilot will integrate remote-sensing validation with in-situ temperature and humidity loggers to quantify seasonal reductions in both surface and near-surface air temperatures. The expectation is that, within two years, these pilots will demonstrate local cooling of 1–2 °C, establishing a replicable model for other wards.

Phase 1: Medium Term (2-6 years) - Ecological and Structural Expansion.

Following successful pilot evaluation, the program should expand toward ecological restoration and material retrofitting across the city. This stage will prioritize the rehabilitation of degraded wetlands and riverbank zones along the Hooghly and in the reclaimed eastern periphery, implemented through partnerships with biodiversity NGOs and local fishing cooperatives (Athukorala et al., 2025; Wang et al., 2022). Concurrently, a city-wide rooftop mandate will be introduced requiring reflective or vegetated roofing for all new commercial buildings, supported by financial incentives and low-interest loans for retrofitting existing low-income dwellings (Budhiyanto et al., 2024). During this period, progress will be tracked through satellite-derived NDVI and albedo metrics, while electricity consumption data from utilities will be analyzed to assess reductions in peak cooling

demand. The integration of nature-based and engineering solutions at this stage is projected to yield measurable surface temperature decreases of 1–3 °C in the most heat-affected neighborhoods.

Phase 2: Long Term (6-15 years) - Institutional Integration and Zoning Reform.

The final phase aims to institutionalize UHI mitigation within the city's urban planning framework and ensure sustained climate resilience. Building on precedents from Guangzhou and other Asian megacities (Luo et al., 2024), ventilation corridors aligned with prevailing Bay-of-Bengal wind directions will be embedded within municipal zoning maps, supported by height and density controls to prevent obstruction of airflow. Simultaneously, peri-urban green belts and blue-green corridors will be legally protected from further encroachment, maintaining the ecological continuity necessary for long-term heat dispersion and stormwater regulation. Integration of UHI performance indicators, like mean April LST and vegetation fraction, into Kolkata's Master Plan and environmental impact assessments will enable periodic evaluation of policy effectiveness. This phase envisions a governance model in which local administrations, research institutions, and citizen groups share data and maintenance responsibilities through an open-access urban climate observatory.

Overall, this phased strategy recognizes that meaningful UHI mitigation requires not only scientific precision but also institutional alignment and public participation. By sequencing rapid demonstration, ecological scaling, and regulatory reform, the framework ensures both immediate temperature relief and durable climate resilience, positioning Kolkata as a model for adaptive urban planning in tropical megacities.

5. Conclusions

This study employed multi-temporal Landsat-derived Land Surface Temperature (LST) and Normalised Difference Vegetation Index (NDVI) datasets processed on the Google Earth Engine (GEE) platform to analyse the spatiotemporal dynamics of the Surface Urban Heat Island (SUHI) effect in Kolkata over a two-decade period (2005–2024). The results unequivocally demonstrate a consistent intensification of surface thermal conditions alongside a progressive decline in vegetative cover, particularly in the pre-monsoon season. High-LST zones, initially localised in industrial, transport, and central commercial areas, have expanded to encompass large peri-urban fringes, while NDVI values indicate the

replacement of vegetated landscapes with impervious surfaces across much of the urban footprint.

The analysis further reveals persistent seasonal asymmetry: April exhibits peak LST values, January remains relatively cooler, and October increasingly sustains elevated post-monsoon temperatures, reflecting diminished thermal recovery. The statistical correlation analysis between LST and NDVI reinforces the inverse relationship between vegetation cover and surface heating, underscoring the role of green infrastructure in mitigating urban heat extremes.

From a sustainability perspective, these findings highlight the urgent need for evidence-based urban planning interventions aimed at reversing vegetation loss, restoring ecological buffers, and incorporating climate-resilient urban design. Without such measures, the trajectory of heat amplification documented here will exacerbate thermal discomfort, public health risks, and energy burdens, undermining Kolkata's long-term habitability.

This research not only provides a robust spatiotemporal benchmark for SUHI monitoring but also reinforces the imperative for integrated, climate-conscious policy frameworks. By leveraging remote sensing-based LST-NDVI analyses, urban managers and planners can identify thermal hotspots, prioritise greening strategies, and align development trajectories with the principles of environmental sustainability and urban resilience.

References

[1] Aboulnaga, M., Trombadore, A., Mostafa, M. and Abouaiana, A., 2024. Livability: The direction to mitigating urban heat islands' effect, achieving healthy, sustainable, and resilient cities, and the coverage. In *Livable cities: Urban heat islands mitigation for climate change adaptation through urban greening* (pp. 1-282). Cham: Springer International Publishing.

[2] Agarwal, V., Kumar, A., Gee, D., Grebby, S., Gomes, R.L. and Marsh, S., 2021. Comparative study of groundwater-induced subsidence for London and Delhi using PSInSAR. *Remote Sensing*, 13(23), p.4741.

[3] Agarwal, V., Kumar, M., Panday, D.P., Zang, J. and Munoz-Arriola, F., 2024. Unlocking the potential of remote sensing for arsenic contamination detection and management: challenges and perspectives. *Current Opinion in Environmental Science & Health*, 42, p.100578.

[4] Ahmad, B., Najar, M.B. and Ahmad, S., 2024. Analysis of LST, NDVI, and UHI patterns for urban climate using Landsat-9 satellite data in Delhi. *Journal of Atmospheric and Solar-Terrestrial Physics*, 265, p.106359.

[5] Almeida, C.R.D., Teodoro, A.C. and Gonçalves, A., 2021. Study of the urban heat island (UHI) using remote sensing data/techniques: A systematic review. *Environments*, 8(10), p.105.

[6] Anand, V., Kaur, S., Rajput, V.D., Minkina, T., Mandzhieva, S., Kumar, S., Sharma, A. and Kumar, S., 2025. Analyzing the spatial relationship between land surface temperature and normalized difference vegetation index using remote sensing and GIS. *Discover Geoscience*, 3(1), p.65.

[7] Basu, J., Sarkar, G., Sarkar, R., Mukhopadhyay, A. and Sikdar, P.K., 2025. Current Status of Climate Vulnerability in Kolkata Urban Agglomeration in the Context of Proposed Resilience and Adaptation. In *India III: Climate Change and Landscape Issues in India: A Cross-Disciplinary Framework* (pp. 407-443). Cham: Springer Nature Switzerland.

[8] Chakraborty, S., Maity, I., Patel, P.P., Dadashpoor, H., Pramanik, S., Follmann, A., Novotný, J. and Roy, U., 2021. Spatio-temporal patterns of urbanization in the Kolkata Urban Agglomeration: A dynamic spatial territory-based approach. *Sustainable Cities and Society*, 67, p.102715.

[9] Chakraborty, S., Maity, I., Patel, P.P., Dadashpoor, H., Pramanik, S., Follmann, A., Novotný, J. and Roy, U., 2021. Spatio-temporal patterns of urbanization in the Kolkata Urban Agglomeration: A dynamic spatial territory-based approach. *Sustainable Cities and Society*, 67, p.102715.

[10] Chatterjee, U. and Majumdar, S., 2022. Impact of land use change and rapid urbanization on urban heat island in Kolkata city: A remote sensing based perspective. *Journal of urban Management*, 11(1), pp.59-71.

[11] Das, A., Agarwal, V. and Kumar, M., 2024. Evaluation of water quality in the Brahmani River basin, Odisha: A multicriteria decision-making approach for sustainable management. In *River Basin Ecohydrology in the Indian Sub-Continent* (pp. 139-165). Elsevier.

[12] Das, S., Choudhury, M.R., Chatterjee, B., Das, P., Bagri, S., Paul, D., Bera, M. and Dutta, S., 2024. Unraveling the urban climate crisis: Exploring the nexus of urbanization, climate change, and their impacts on the environment and human well-being—A global perspective. *AIMS Public Health*, 11(3), p.963.

[13] Halder, B., Bandyopadhyay, J. and Banik, P., 2021. Monitoring the effect of urban development on urban heat island based on remote sensing and geo-spatial approach in Kolkata and adjacent areas, India. *Sustainable Cities and Society*, 74, p.103186.

[14] Hemati, M., Hasanolou, M., Mahdianpari, M. and Mohammadimanesh, F., 2021. A systematic review of landsat data for change detection applications: 50 years of monitoring the earth. *Remote sensing*, 13(15), p.2869.

[15] Hossain, A.K.M. and Easson, G., 2015. Potential impacts of the growth of a Mega City in Southeast Asia, a case study on the City of Dhaka, Bangladesh. In *Handbook of Climate Change Mitigation and Adaptation* (pp. 1-24). Springer, New York, NY.

[16] Islam, S., Karipot, A., Bhawar, R., Sinha, P., Kedia, S. and Khare, M., 2024. Urban heat island effect in India: a review of current status, impact and mitigation strategies. *Discover Cities*, 1(1), p.34.

[17] Jabbar, H.K., Hamoodi, M.N. and Al-Hameedawi, A.N., 2023. Urban heat islands: a review of contributing factors, effects and data. In *IOP Conference Series: Earth and Environmental Science* (Vol. 1129, No. 1, p. 012038). IOP Publishing.

[18] Jayasinghe, C.B., Withanage, N.C., Mishra, P.K., Abdelrahman, K. and Fnais, M.S., 2024. Evaluating Urban Heat Islands Dynamics and Environmental

Criticality in a Growing City of a Tropical Country Using Remote-Sensing Indices: The Example of Matara City, Sri Lanka. *Sustainability*, 16(23), p.10635.

[19] Joshi, K., Khan, A., Anand, P. and Sen, J., 2024. Understanding the synergy between heat waves and the built environment: a three-decade systematic review informing policies for mitigating urban heat island in cities. *Sustainable Earth Reviews*, 7(1), p.25.

[20] Joshi, K., Khan, A., Anand, P. and Sen, J., 2024. Understanding the synergy between heat waves and the built environment: a three-decade systematic review informing policies for mitigating urban heat island in cities. *Sustainable Earth Reviews*, 7(1), p.25.

[21] Kotharkar, R., Ramesh, A. and Bagade, A., 2018. Urban heat island studies in South Asia: A critical review. *Urban climate*, 24, pp.1011-1026.

[22] Kumar, A., Agarwal, V., Pal, L., Chandniha, S.K. and Mishra, V., 2021. Effect of land surface temperature on urban heat island in Varanasi City, India. *J*, 4(3), pp.420-429.

[23] Li, Z.L., Wu, H., Duan, S.B., Zhao, W., Ren, H., Liu, X., Leng, P., Tang, R., Ye, X., Zhu, J. and Sun, Y., 2023. Satellite remote sensing of global land surface temperature: Definition, methods, products, and applications. *Reviews of Geophysics*, 61(1).

[24] Maity, S., Das, S., Pattanayak, J.M., Bera, B. and Shit, P.K., 2022. Assessment of ecological environment quality in Kolkata urban agglomeration, India. *Urban Ecosystems*, 25(4), pp.1137-1154.

[25] Maltare, N.N., Vahora, S. and Jani, K., 2024. Seasonal analysis of meteorological parameters and air pollutant concentrations in Kolkata: An evaluation of their relationship. *Journal of Cleaner Production*, 436, p.140514.

[26] Mohanasundaram, S., Baghel, T., Thakur, V., Udmale, P. and Shrestha, S., 2023. Reconstructing NDVI and land surface temperature for cloud cover pixels of Landsat-8 images for assessing vegetation health index in the Northeast region of Thailand. *Environmental monitoring and assessment*, 195(1), p.211.

[27] Mondal, D. and Banerjee, A., 2021. Exploring peri-urban dynamism in India: Evidence from Kolkata Metropolis. *Journal of Urban Management*, 10(4), pp.382-392.

[28] Oke, T.R., 1995. The heat island of the urban boundary layer: characteristics, causes and effects. In *Wind climate in cities* (pp. 81-107). Dordrecht: Springer Netherlands.

[29] Panday, D.P., Agarwal, V. and Kumar, M., 2025. Statistical variability of precipitation and the detection approaches. In *Water Sustainability and Hydrological Extremes* (pp. 77-88). Elsevier.

[30] Panday, D.P., Kumar, M., Agarwal, V., Torres-Martínez, J.A. and Mahlknecht, J., 2024. Corroboration of arsenic variation over the Indian Peninsula through standardized precipitation evapotranspiration indices and groundwater level fluctuations: Water quantity indicators for water quality prediction. *Science of the Total Environment*, 954, p.176339.

[31] Raufu, I.O., 2024. Exploring the relationship between remote sensing-based vegetation indices and land surface temperature through quantitative analysis. *Journal of the Bulgarian Geographical Society*, 50, pp.95-112.

[32] Ren, Y., Laforteza, R., Giannico, V., Sanesi, G., Zhang, X. and Xu, C., 2023. The unrelenting global expansion of the urban heat island over the last century. *Science of The Total Environment*, 880, p.163276.

[33] Sarif, M.O., Ranagalage, M., Gupta, R.D. and Murayama, Y., 2022. Monitoring urbanization induced surface urban cool island formation in a South Asian Megacity: a case study of Bengaluru, India (1989–2019). *Frontiers in Ecology and Evolution*, 10, p.901156.

[34] Shahfahad, Talukdar, S., Rihan, M., Hang, H.T., Bhaskaran, S. and Rahman, A., 2022. Modelling urban heat island (UHI) and thermal field variation and their relationship with land use indices over Delhi and Mumbai metro cities. *Environment, Development and Sustainability*, 24(3), pp.3762-3790.

[35] Shen, P., Zhao, S. and Ma, Y., 2021. Perturbation of urbanization to Earth's surface energy balance. *Journal of Geophysical Research: Atmospheres*, 126(8), p.e2020JD033521.

[36] Shen, P., Zhao, S., Ma, Y. and Liu, S., 2023. Urbanization-induced Earth's surface energy alteration and warming: A global spatiotemporal analysis. *Remote Sensing of Environment*, 284, p.113361.

[37] Shi, H., Xian, G., Auch, R., Gallo, K. and Zhou, Q., 2021. Urban heat island and its regional impacts using remotely sensed thermal data—a review of recent developments and methodology. *Land*, 10(8), p.867.

[38] Singh, B.V.R., Batar, A.K., Agarwal, V., Sen, A. and Kulhari, K., 2025. Forest fragmentation and human-wildlife conflict: assessing the impact of land use land cover change in Ranthambore Tiger Reserve, India. *Environmental Research Communications*, 7(6), p.061006.

[39] Tabassum, A., Kamal, A.M., Rahman, M.Z. and Shahid, S., 2025. Impact of urban sprawl on urban heat island in Chittagong: a non-parametric analysis using satellite nighttime light and land surface temperature data for the period 2000–2021: Tabassum et al. *Theoretical and Applied Climatology*, 156(6), p.341.

[40] Taloor, A.K., Parsad, G., Jabeen, S.F., Sharma, M., Choudhary, R. and Kumar, A., 2024. Analytical study of land surface temperature for evaluation of UHI and UHS in the city of Chandigarh India. *Remote Sensing Applications: Society and Environment*, 35, p.101206.

[41] Vishvendra Raj Singh, B., Agarwal, V. and Sanwal, V., 2024. Climatic shifts and vegetation response in Western India: a four-decade retrospective through GIS and multi-variable analysis. *Oxford Open Climate Change*, 4(1), p.kgae020.

[42] Voogt, J.A. and Oke, T.R., 2003. Thermal remote sensing of urban climates. *Remote sensing of environment*, 86(3), pp.370-384.

[43] Wulder, M.A., Roy, D.P., Radeloff, V.C., Loveland, T.R., Anderson, M.C., Johnson, D.M., Healey, S., Zhu, Z., Scambos, T.A., Pahlevan, N. and Hansen, M., 2022. Fifty years of Landsat science and impacts. *Remote Sensing of Environment*, 280, p.113195.

[44] Athukorala, D., Murayama, Y., Herath, N. S. K., Madduma Bandara, C. M., Singh, R. K., & Fernando, S. L. J. (2025). Exploring the cooling effects of urban

wetlands in Colombo City, Sri Lanka. *Remote Sensing*, 17(11), 1919. <https://doi.org/10.3390/rs17111919>

[45] Budhiyanto, A. C. A., Wibowo, Y. E., & Yuliastuti, N. (2024). A comparative study of cool roof and green roof thermal performance in tropical climates. *Journal of Architectural Research and Design Studies*, 8(2), 119–135.

[46] Cheela, V. R. S., Kothuru, S., & Madduru, S. R. (2021). Combating the Urban Heat Island effect: A review of reflective pavements. *Buildings*, 11(3), 93. <https://doi.org/10.3390/buildings11030093>

[47] Li, H., Ren, Y., Laforteza, R., Giannico, V., Sanesi, G., & Xu, C. (2024). Cooling efficacy of trees across cities is determined by tree traits, morphology, and climate. *Communications Earth & Environment*, 5, 315. <https://doi.org/10.1038/s43247-024-01908-4>

[48] Luo, Y., Huang, Z., & Ding, W. (2024). Simulating the impact of ventilation corridors on urban thermal environments in Guangzhou using LCZ-based ENVI-met and least-cost path analysis. *Energy and Buildings*, 307, 113040. <https://doi.org/10.1016/j.enbuild.2024.113040>

[49] Priya, U. K., Balaji, N., & Ramakrishnan, K. (2024). Enhancing sustainable thermal comfort of tropical urban apartments via balcony plants: A case study of Chennai, India. *Buildings*, 14(8), 2353. <https://doi.org/10.3390/buildings14082353>

[50] Wang, Y., Li, Y., & Chen, Y. (2022). The cooling effect of an urban river and its interaction with littoral built environment. *Sustainability*, 14(18), 11700. <https://doi.org/10.3390/su141811700>

[51] Xie, M., Zhang, Y., & Chen, F. (2016). Modeling anthropogenic heat flux and its impact on regional climate: A study for Shanghai. *Atmospheric Chemistry and Physics*, 16(10), 6071–6089. <https://doi.org/10.5194/acp-16-6071-2016>

[52] Zaki, S. A., Choon, S. W., & Zakaria, R. (2020). Effects of roadside trees and road orientation on the outdoor thermal environment in Kuala Lumpur, Malaysia. *Sustainability*, 12(3), 1053. <https://doi.org/10.3390/su12031053>

APPENDIX

Google Earth Engine code for Landsat 8

// 1. Define Kolkata boundary using GAUL dataset

```
var kolkata = ee.FeatureCollection("FAO/GAUL/2015/level2")
.filter(ee.Filter.eq('ADM2_NAME', 'Kolkata'));
Map.centerObject(kolkata, 10);
Map.addLayer(kolkata, {color: 'black'}, 'Kolkata');
```

// 2. Load Landsat 8 SR dataset

```
var landsat = ee.ImageCollection("LANDSAT/LC08/C02/T1_L2")
.filterBounds(kolkata)
.filterDate('2024-01-1', '2024-01-31')
.filterMetadata('CLOUD_COVER', 'less_than', 10);
```

// 3. Select the least cloudy image

```
var image = ee.Image(landsat.sort('CLOUD_COVER').first()).clip(kolkata); print("Selected Landsat Image", image);
print("Image Acquisition Date:", image.get('DATE_ACQUIRED'));
```

// 4. Convert DN to Top-of-Atmosphere (TOA) Reflectance and Brightness Temperature using scale factors from USGS documentation

```
var toa = image.multiply(0.0000275).add(-0.2);
var thermal = image.select('ST_B10').multiply(0.00341802).add(149.0); // Kelvin
```

// 5. NDVI = (NIR - RED) / (NIR + RED)

```
var ndvi = image.normalizedDifference(['SR_B5', 'SR_B4']).rename('NDVI');
```

// 6. Calculate LST from Thermal band (B10)

//Basic LST estimation assuming land emissivity ~ 0.98, Converting Kelvin to Celsius

```
var lst = thermal.subtract(273.15).rename('LST_Celsius');
```

// Computing zonal statistics over Kolkata

```
var stats = lst.reduceRegion({ reducer: ee.Reducer.mean()
.combine(ee.Reducer.median(), ", true")
.combine(ee.Reducer.max(), ", true) .combine(ee.Reducer.min(), ", true), geometry: kolkata.geometry(), scale: 30, maxPixels: 1e9
});
```

```
print('LST Stats: ', stats);
```

```
var statsn = ndvi.reduceRegion({ reducer: ee.Reducer.mean()
.combine(ee.Reducer.median(), ", true")
.combine(ee.Reducer.max(), ", true) .combine(ee.Reducer.min(), ", true), geometry: kolkata.geometry(), scale: 30, maxPixels: 1e9
});
```

```
});
```

```
print('NDVI Stats', statsn);
```

// 7. Setting Visualization parameters

var ndviParams = {min: 0, max: 1, palette: ['white', 'black']}; var lstParams = {min: 20, max: 45, palette: ['blue', 'yellow', 'red']};

// 8. Adding to map

```
Map.addLayer(ndvi, ndviParams, 'NDVI');
Export.image.toDrive({image: lst, description:'ndvi', folder: 'GEE_Exports', // This is the target folder in Google Drive
fileNamePrefix: 'Kolkata_NDVI_', region: kolkata.geometry(), scale: 30, maxPixels: 1e9
});
Map.addLayer(lst, lstParams, 'Land Surface Temperature (°C)');
Export.image.toDrive({ image: lst, description:'lst', folder: 'GEE_Exports', fileNamePrefix: 'Kolkata_LST_', region: kolkata.geometry(), scale: 30, maxPixels: 1e9});
```

Statistical summary of LST

Year	Category	Winter (Jan)	Summer (April)	Monsoon (July)	Post-Monsoon (October)
2005	Image Date	2005- 01- 15	2005- 03- 04	2005-06- 08	2005- 10- 14
	mean	24.70182843	37.75416408	-28.06186046	37.22598387
	median	24.53058475	37.9365401	-28.48828091	37.31403029
	max	31.86210488	47.2807931	36.11070374	50.60310854
	min	20.16222242	24.83123774	-104.8621131	24.51336188
2010	Image Date	2010-01- 29	2010- 04- 03	2010- 08- 09	2010- 10- 28
	mean	26.69881079	30.87979262	14.80301781	34.53628458
	median	26.80951941	31.56380315	14.12494102	34.56240426
	max	34.22053868	44.55321314	52.25743022	43.63718378
	min	17.53376504	20.33654144	-21.81106318	26.8581236
2015	Image Date	2015- 01- 19	2015- 04- 25	2015- 07- 14	2015- 10- 18
	mean	15.6267817	34.13564683	-63.15294862	38.60681164
	median	15.34474304	35.68618461	-54.51657907	39.81187081
	max	22.30532096	47.73538976	34.80160208	49.41363758
	min	10.6054385	17.9712716	-123.1485201	19.40000396
2020	Image Date				
	mean	28.78361945	46.15652218	data unavailable	33.96249337
	median	28.84440495	46.56312673		36.12787947
	max	36.15855602	56.834159		50.07673346
	min	20.3809757	31.68436784		5.85097268
2024	Image Date	2024- 01- 12	2024- 04- 01	data unavailable	2024- 10- 10
	mean	23.875943	42.89620792		39.80901438
	median	23.84399133	43.06331257		40.06170893
	max	29.39771246	50.91756638		47.7251357
	min	19.75889606	31.199009		31.2160991

Statistical summary of NDVI

Year	Category	Winter (Jan)	Summer (April)	Monsoon (July)	Post-Monsoon (October)
2005	max	0.241877516	0.399743614	0.29074534	0.451538336
	mean	0.039993732	0.081539219	0.042552261	0.135425067
	median	0.034271388	0.071336699	0.080124718	0.123014559
	min	-0.043928604	-0.089085726	-0.455217667	-0.440915537
2010	max	0.297660546	0.2845378	0.348056818	0.438046647
	mean	0.054744444	0.063581462	-0.100216517	0.126836967
	median	0.049697719	0.052659401	1.1748E-05	0.115215317
	min	-0.094194072	-0.332702925	-0.503544635	-0.087657849
2015	max	0.483826957	0.446066174	0.429389137	0.548951049
	mean	0.064190796	0.124875031	0.137323042	0.129080044
	median	0.048781488	0.116210955	0.133766596	0.119112625
	min	-0.017806187	-0.045087336	-0.043444888	-0.090589888
2020	max	0.371643534	0.527645839	data unavailable	0.815865511
	mean	0.089108622	0.13884054		0.123620966
	median	0.081041409	0.123027446		0.113299649
	min	-0.06448039	-0.110555456		-0.196686976
2024	max	0.416069155	0.475979576	data unavailable	0.439414115
	mean	0.092799947	0.135049823		0.175530466
	median	0.08396811	0.123019987		0.165015088
	min	-0.089331982	-0.06010929		-0.023160702